Supplemental File

Title: Topical, immunomodulatory epoxy-tiglianes induce biofilm disruption and healing in acute and chronic skin wounds‡

Authors: Lydia C. Powell[1,2*†], Jason K. Cullen[3,8†], Glen M. Boyle[3,8], Tom De Ridder[4], Pei-Yi Yap[3], Wenya Xue[1], Carly J. Pierce[3], Manon F. Pritchard[1], Georgina E. Menzies[5], Muthanna Abdulkarim[6], Jennifer Y. M. Adams[1], Joana Stokniene[1], Lewis W. Francis[2], Mark Gumbleton[6], Jenny Johns[3], Katja E. Hill[1], Adam V. Jones[7], Peter G. Parsons[3], Paul Reddell[4], David W. Thomas[1].

Affiliations:

[1]Advanced Therapies Group, Cardiff University School of Dentistry; Cardiff, CF14 4XY, UK.

[2]Centre for Nanohealth, Swansea University Medical School, Swansea University; Swansea SA2 8PP, UK.

[3]Drug Discovery Group, QIMR Berghofer Medical Research Institute; Brisbane, 4006, Australia.

[4]QBiotics Group Limited; Yungaburra, 4884, Australia.

[5]School of Biosciences, Cardiff University; Cardiff, CF10 3AX, UK.

[6]School of Pharmacy and Pharmaceutical Sciences, Cardiff University; Cardiff, CF10 3NB, UK.

[7]Oral Pathology, Cardiff and Vale University Health Board; Cardiff, CF14 4XY, UK.

[8]School of Biomedical Sciences, Faculty of Medicine, University of Queensland; Brisbane, 4072, Australia

[*]Corresponding author. Email: Powelllc1@cardiff.ac.uk

[†]These authors contributed equally to this work.

MATERIALS AND METHODS

Observational canine study

An observational study of EBC-46 treatment of a non-healing, soft-tissue wound present on a 3 year-old canine was performed. The wound was previously unresponsive to standard treatment protocols (antibiotic and anti-inflammatory therapies) over a period of > 12 weeks. Treatment involved topical application of EBC-46 (3 mg/ml; days 1, 2, 6, 10 and 14) and, at day 28, a single, subcutaneous injection of EBC-46 (0.5 mg/ml) at the periphery of the healing wound. The formulation of the topical gel was 0.3% w/w carbomer 940 in 50% v/v isopropanol. Photographs of the canine wound were taken at various times post treatment.

Motility studies

Overnight cultures of *P. aeruginosa* PAO1 were adjusted in TSB to OD_{600} = 0.08, before adding 10 µl of bacteria to 90 µl TSB ± EBC-1013, EBC-46, EBC-147 or vehicle (ethanol) equivalent at a concentration of 256 µg/ml. The PAO1 cells were then shaken at 60 rpm for 1.5 h (37°C). Swarming motility was evaluated on Basal medium 2 glucose agar (BM2; 0.5% agar [Sigma-Aldrich], 62 mM potassium phosphate buffer [pH 7], 2 mM $MgSO_4$, 10 µM $FeSO_4$, 0.4% [wt/vol] glucose, 0.5% [wt/vol] casamino acids) within 6-well plates (*78*). Swarming colony formation was assessed by spotting 1 µl of bacteria in epoxy-tiglianes or untreated and vehicle (ethanol) controls onto the centre of each agar well. The bacterial drops were allowed to dry for 10 min, until the inoculate was absorbed into the agar. Photographic images of colony growth, with incubation at 37°C, were taken at 12, 14, 16 and 18 h intervals and the images analyzed by ImageJ software to obtain surface area and circularity measurements (n=3). Circularity was calculated using the formula: circularity = $4\pi(\text{area}/\text{perimeter}^2)$, with a circularity value of 1 indicating a perfect circle, whilst a value approaching 0, was an indication of an increasingly elongated polygon.

Hydrophobicity studies

An overnight culture of *E. coli* IR57 was adjusted to OD_{625} of 0.1 (4×10^7 cfu/ml) in MH broth and incubated ± EBC-1013, EBC-147, EBC-46 or vehicle (ethanol) equivalent (256 µg/ml) at 37°C for 1 h (shaken 120 rpm). Bacterial lawns were prepared as previously described by Soon et al. (*79*). Bacteria were first collected by centrifugation (3000 *g*, 5 min), washed twice and resuspended in Milli-Q water. Bacterial lawns were prepared by filtering 10 ml of bacterial suspension through 0.22 µm pore size Durapore polyvinylidene difluoride membrane filters (PVDF, Millipore) until all the fluid passed through. Filters were air-dried in a laminar flow cabinet for 15 min, mounted onto glass slides with double-sided adhesive tape and further air-dried for 15 min. Contact angles of Milli-Q water (5 µl) were measured using the sessile drop method with an Attension Theta Lite contact meter (Biolin Scientific). Contact angles (20 images/s) were obtained immediately after the deposition of the drop on *E. coli* IR57 lawns (or filter only controls) and recorded over a 10 s interval ($n \geq 3$).

Multiple particle tracking (MPT)

Established (48 h) *E. coli* IR57 biofilms were grown and then treated with EBC-46, EBC-1013 or EBC-147 (256 µg/ml), being incubated for a further 24 h before MPT measurement. Negatively charged carboxylate-modified 200 nm *Fluo*spheres ([Ex/Em]: [580/605 nm]; ThermoFisher Scientific) were used in this study and characterized in PBS buffer through zeta potential and sizing measurements using a Malvern Zetasizer Nano ZS prior to MPT studies. The *Fluo*spheres suspension was vortexed for 1 min, then diluted in sterilized PBS buffer (0.0025%), before addition of 10 µl diluted *Fluo*spheres suspension onto the biofilms followed by a 2 h incubation. Biofilms were stained with SYTO 9 before addition of the *Fluo*spheres to visualize the lower layers of the biofilm matrix using a Leica DM IRB wide-field Epifluorescence microscope (×63 oil immersion lens). Videos of particle movement within the biofilms were captured at a frame rate of 33 ms (600 frames, 20 s) using a high speed

camera (Allied Vision Technologies, UK) and then particle trajectories were tracked using ImageJ software (Mosaic) over 2 s to convert nanoparticle movements into metric displacements in both the X and Y directions. Ensemble mean square displacement ‹MSD›, effective diffusion coefficient ‹Deff›, and heterogeneity of particle diffusion were measured as previously described (*30*). Here, 120 particle movements were captured in each biofilm well, and each bacterial strain was tested in triplicate (i.e. 360 particles in total for each biofilm species). The viscoelastic properties of the biofilms were assessed by determining the anomalous diffusion exponent (α) as follows. This was calculated by fitting the power law to log(‹MSD›) versus log(Δt) and calculating the slope of this data, where $\alpha = 1$ for a completely viscous system (liquid), $\alpha = 0$ for a completely elastic system (solid) and $1 > \alpha > 0$ for a viscoelastic system. Additionally, the micro-rheological properties of the biofilms were further defined by calculation of the creep compliance (J(t)), where the MSD represents deformation of the biofilm within time (Δt) under constant pressure/shear force represented by the temperature of the atmosphere. Creep compliance (J(T)) was calculated by the following equation: [$J(t)= 3\pi d/4\kappa T<MSD(t)$] where κ is the Boltzmann constant, T is absolute temperature and d is the diameter of the particle in μm.

Zeta Potential (surface charge) assay

The zeta potential of planktonic cultures of *E.coli* IR57 cells treated for 24 h (37^{o}C) with 256 μg/ml epoxy-tiglianes (EBC-46 and ECB-1013), together with vehicle (ethanol) and untreated controls, were assessed. Firstly, bacterial cultures ± treatment were washed twice through centrifugation (3,400 *g*, 5 min) and the resultant bacterial pellets were resuspended in 1 mM NaCl in deionised water (pH 7). The bacterial solutions were then placed into disposable capillary cells (DTS1061; Malvern Instruments) and a Zetasizer Nano ZS (Malvern Instruments) was used for zeta potential measurement. The Smoluchowski's model was applied for zeta potential calculation.

Reactive oxygen species (ROS) assays

PMNLs (n=4 human donors: 2 male, 2 female) were resuspended in HBSS, 2% FCS at a concentration of 2.2×10^6 cells/ml. Then, 45 µl of unstained cell suspension (100,000 cells) was aliquoted into 3 wells in a black, half volume 96-well plate (Greiner #675077) as controls for background fluorescence. Dihydroethidium (DHE) was then added to the remaining cell suspension (5 µg/ml final concentration) and 45 µl of stained cells plated into the same half area 96-well plate. Serial dilutions of PMA and EBC-1013 (10× final assay concentration) were prepared in HBSS, 2% FCS, after which 10 µl of each dilution was added to the required wells in duplicate. DHE fluorescence (Ex: 485/20 nm; Em: 620/40 nm) was measured in each well after 30 min incubation (37°C, 5% CO_2) using a Hybrid H4 Synergy plate reader (BioTek). Fluorescence values (after background fluorescence subtraction) were expressed as mean RFU or converted to mean % ROS production values (based on the maximal DHE fluorescence signal from PMA-treated samples). Mean % ROS production values ± SD were plotted versus $\log_{10}$[EBC-1013] and absolute EC_{50} values and 95% confidence intervals determined using the following algorithm in GraphPad PRISM v8.4:

$$Y = Bottom + (100 - Bottom)/(1 + 10\text{^}((LogEC50 - X) * HillSlope + log((100 - Bottom)/(50 - Bottom) - 1)))$$

Cellular viability assays

Cells were plated into either clear, flat bottom 96-well plates (HaCaT and HDF, 10,000 cells per well) or clear U-bottom 96-well plates (PBMCs from 3 distinct donors, 2 male, 1 female; 150,000 cells per well) and incubated overnight at 37°C, 5% CO_2 overnight. After 24 h, EBC-1013 was prepared in complete media and added to the required wells at the following (final) concentrations: 1, 0.1 and 0.01 µg/ml. Vehicle-only controls (ethanol) were also compiled. Plates were incubated for 72 h as above and cell viability determined using CellTiter-Glo 3D

reagent (Promega) according to the manufacturer's instructions. Luminescent signal in each well was determined using a Hybrid Synergy H4 plate reader (Bio-Tek). Luminescent signals from compound-treated wells were normalized to vehicle-treated wells and were expressed as % survival.

Histological and immunohistochemical analysis

Tissue samples (from the acute wound model in calves and efficacy/kinetic experiments in *db/db* mice) were fixed in 10% neutral-buffered formalin solution and processed. An alphanumeric code was used to blind researchers to treatment groups and 4 µm thick sections prepared from paraffin embedded tissue blocks. Sections were de-paraffinized for 3 min at each stage in the following solutions: xylene, xylene and ethanol at concentrations of 100%, 100%, 95%, 70%, 50% and rehydrated in double distilled water. The tissue sections were then rehydrated in double distilled water before being stained with conventional hematoxylin and eosin (H&E), Masson trichome and van Gieson stains (*80*). Conventional hematoxylin and eosin (H&E) staining was performed in a Shandon Linistain (ThermoFisher Scientific) and comprised Harris haematoxylin (2 min), H_2O (1 min), 5% acetic acid in 70% ethanol (30 s), H_2O (1 min), Scotts tap H_2O substitute (30 s), H_2O (30 s), aqueous eosin Y (1 min), H_2O (30 s), 95% ethanol (30 s), 100% ethanol (2 min), ethanol/xylene (50/50 mix; 30 s) and xylene (1 min). Masson trichome and van Gieson stains were prepared as per standard protocols (*80*). H&E and trichome-stained sections were assessed subjectively under standard light microscopy. The degree of ulceration, presence of granulation tissue, remodeled collagen and inflammation were scored from 0 to 4: where 0 = no presence, 1 = <25%, 2 = 25-50%, 3 = 50-75% and 4 = >75%. Surface bacterial colonization was scored as: 0 (no presence), 1 (minimal), 2 (scattered colonies), 3 (moderate) and 4 (widespread colonization). For immunohistochemical staining, deparaffinized and rehydrated sections were treated with 1.0% H_2O_2 in tris buffered saline (TBS) pH 7.6 to block endogenous peroxidase activity, then antigen

retrieval was performed at 100°C using a Biocare Medical Decloaking Chamber and Diva Decloaker solution (Biocare Medical). Slides were blocked with Background Sniper (Biocare Medical) and then incubated with anti-Ly6G (Abcam, #ab2557) overnight at room temperature. Following TBS washes, Rat Probe (Biocare Medical) was added and Rat HRP Polymer and Betazoid DAB staining (Biocare Medical) performed. Sections were counterstained with haematoxylin prior to imaging.

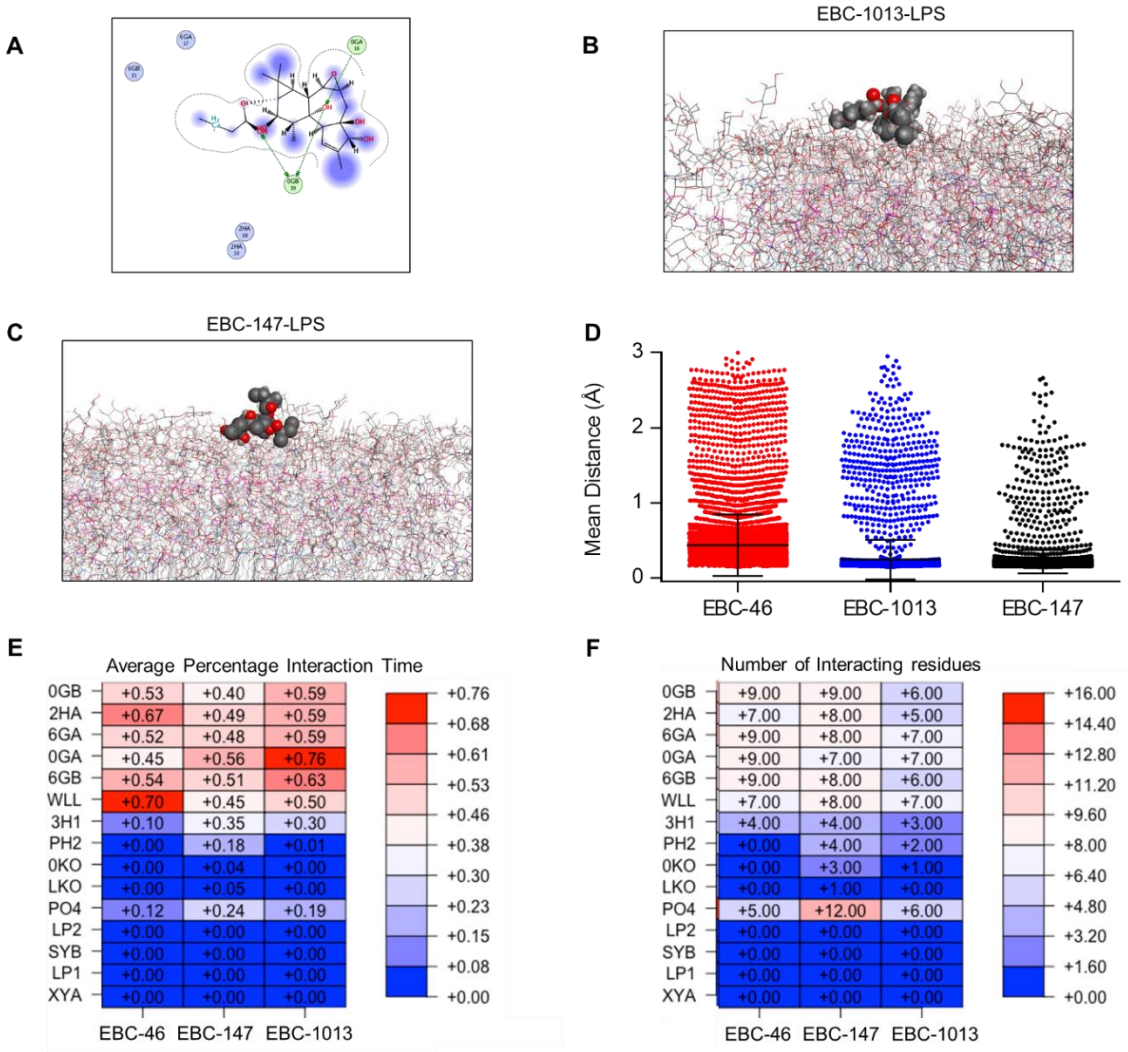
A
B
EBC-1013-LPS
C
EBC-147-LPS
D
Mean Distance (Å)
3
2
1
0
EBC-46
EBC-1013
EBC-147
E
Average Percentage Interaction Time
0GB +0.53 +0.40 +0.59
2HA +0.67 +0.49 +0.59
6GA +0.52 +0.48 +0.59
0GA +0.45 +0.56 +0.76
6GB +0.54 +0.51 +0.63
WLL +0.70 +0.45 +0.50
3H1 +0.10 +0.35 +0.30
PH2 +0.00 +0.18 +0.01
0KO +0.00 +0.04 +0.00
LKO +0.00 +0.05 +0.00
PO4 +0.12 +0.24 +0.19
LP2 +0.00 +0.00 +0.00
SYB +0.00 +0.00 +0.00
LP1 +0.00 +0.00 +0.00
XYA +0.00 +0.00 +0.00
EBC-46 EBC-147 EBC-1013
+0.76
+0.68
+0.61
+0.53
+0.46
+0.38
+0.30
+0.23
+0.15
+0.08
+0.00
F
Number of Interacting residues
0GB +9.00 +9.00 +6.00
2HA +7.00 +8.00 +5.00
6GA +9.00 +8.00 +7.00
0GA +9.00 +7.00 +7.00
6GB +9.00 +8.00 +6.00
WLL +7.00 +8.00 +7.00
3H1 +4.00 +4.00 +3.00
PH2 +0.00 +4.00 +2.00
0KO +0.00 +3.00 +1.00
LKO +0.00 +1.00 +0.00
PO4 +5.00 +12.00 +6.00
LP2 +0.00 +0.00 +0.00
SYB +0.00 +0.00 +0.00
LP1 +0.00 +0.00 +0.00
XYA +0.00 +0.00 +0.00
EBC-46 EBC-147 EBC-1013
+16.00
+14.40
+12.80
+11.20
+9.60
+8.00
+6.40
+4.80
+3.20
+1.60
+0.00
G
Log P (lipophilicity)
3
2
1
0
EBC-46
EBC-1013
EBC-147

Fig. S1. Molecular dynamics simulations showing the interaction of epoxy-tiglianes with the *P. aeruginosa* PAO1 cell outer membrane (LPS-DPPE) bilayer. (**A**) A single time point showing EBC-46 bonds with the LPS residues through hydrogen bonding, in this case bonding with 0GA and 0GB. (Various interactions like this are made throughout the simulation). (**B-C**) Molecular representation of EBC-1013 and EBC-147 interaction within the *P. aeruginosa* PAO1 cell outer membrane (LPS-DPPE) bilayer. (**D**) Mean distance between the LPS and EBC compounds during the simulation, showing differing interactions between the surface and the compounds. Results are expressed in Angstroms (Å). The scatter dot plot shows mean values ± SD. (**E**) Average Percentage Interaction times and (**F**) Number of Interacting Residues contact maps produced by CONAN showing the number and length of interactions with specific residues. LPS residues are listed down the left-hand side, 0-β-D-glucose [0GB], 2-α-L-rhamnose [2HA], 6-α-D-glucose [6GA], 0-α-D- glucose [0GA], 6-β-D-glucose [6GB], 2-(2-L-alanyl)-2-deoxy-D-galactosamine [WLL], L-glycero-D-mannoheptose-7-formamide [3H1], 2-(2-hydroxyethyl)-6-deoxy-D-manno-heptose [PH2], 3-deoxy-D-manno-oct-2-ulosonic acid [0KO and variant LKO], phosphate [PO4], 3-hydroxydecanoyl acid 10:0 (3-OH) [LP2], dodecanoyl acid (12:0) [LP1], 3-(acetyl amino)-3-deoxy-D-glucose [XYA and variant SYB] with surface residues (EBC compounds) at the bottom. (**G**) Octanol–water partition coefficient (lipophilicity) of the epoxy-tigliane compounds, as calculated by Swiss ADME computational chemistry website. Results are expressed as Log *P*.

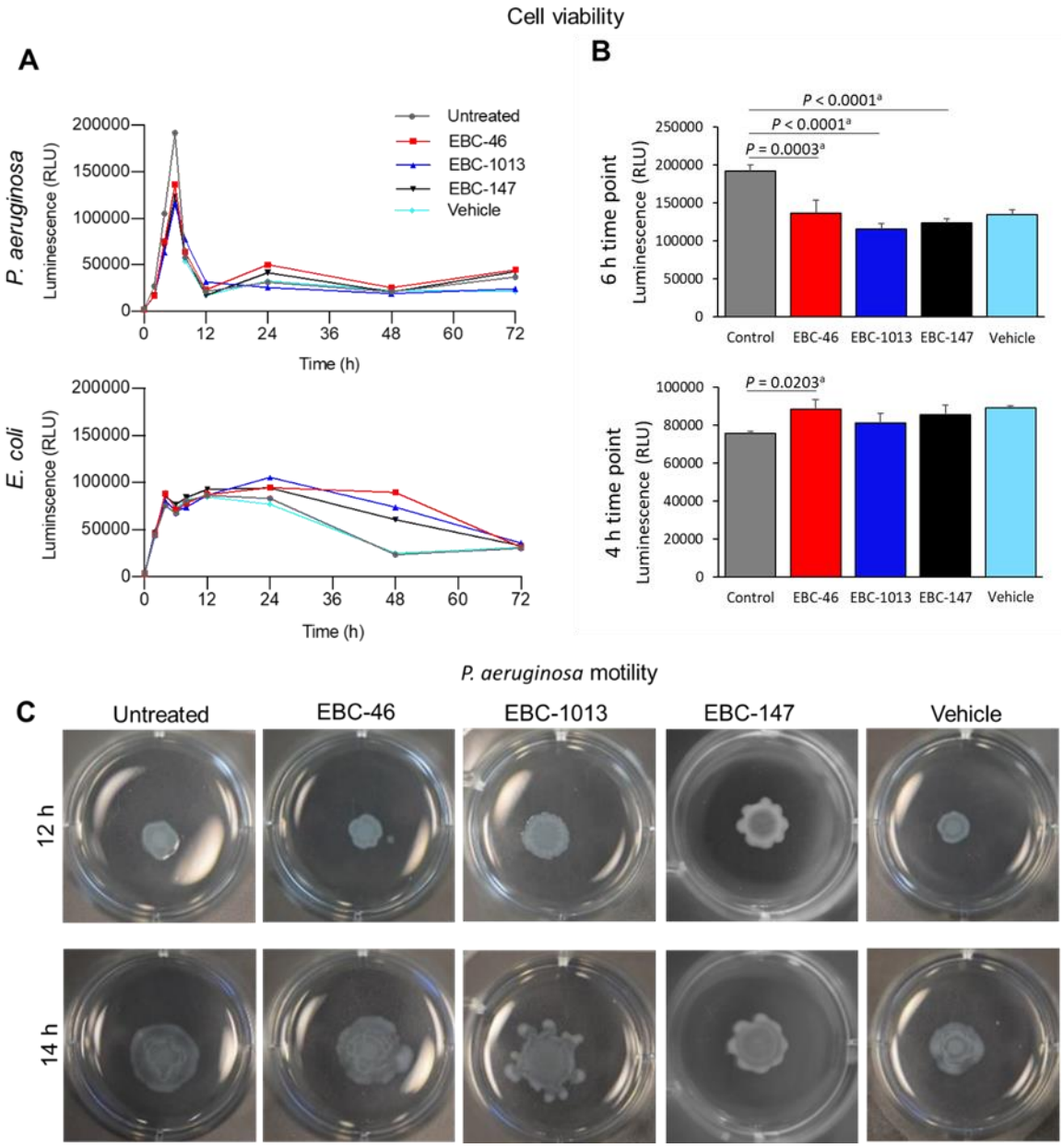
Cell viability
A
P. aeruginosa
Luminescence (RLU)
200000
150000
100000
50000
0
0
12
24
36
48
60
72
Time (h)
Untreated
EBC-46
EBC-1013
EBC-147
Vehicle
E. coli
Luminscence (RLU)
Time (h)
B
6 h time point
Luminescence (RLU)
P < 0.0001a
P < 0.0001a
P = 0.0003a
250000
200000
150000
100000
50000
0
Control
EBC-46
EBC-1013
EBC-147
Vehicle
4 h time point
Luminescence (RLU)
P = 0.0203a
100000
80000
60000
40000
20000
0
P. aeruginosa motility
C
Untreated
EBC-46
EBC-1013
EBC-147
Vehicle
12 h
14 h

Fig. S2. **The effect of epoxy-tiglianes treatment on bacterial growth and motility in Gram-negative bacteria**. (**A**) ATP cell viability assay of Gram-negative strains (*P. aeruginosa* PAO1, *E. coli* IR57) ± epoxy-tigliane treatment (EBC-46, EBC-1013, EBC-147 and untreated and vehicle controls at 256 µg/ml. Results are expressed as mean RLU (relative light unit; n=3). (**B**) Graphs of ATP cell viability assay from maximum growth of Gram-negative strains (*P. aeruginosa* PAO1 and *E. coli* IR57 at 6 h and 4 h time points respectively) ± epoxy-tigliane treatment and untreated and vehicle control at 256 µg/ml (n=3). Data shown as mean ±SD. Statistical comparisons were made using one way ANOVA with Tukey's multiple comparisons test (n=3). [a]Indicates no significant difference between EBC-treated and vehicle control measurements ($P > 0.05$). (**C**) Bacterial swarming motility images over time (12 and 14 h) of *P. aeruginosa* PAO1 on BM2 medium ± 256 µg/ml epoxy-tigliane treatment (EBC-1013, EBC-46 and EBC-147) and untreated and vehicle controls.

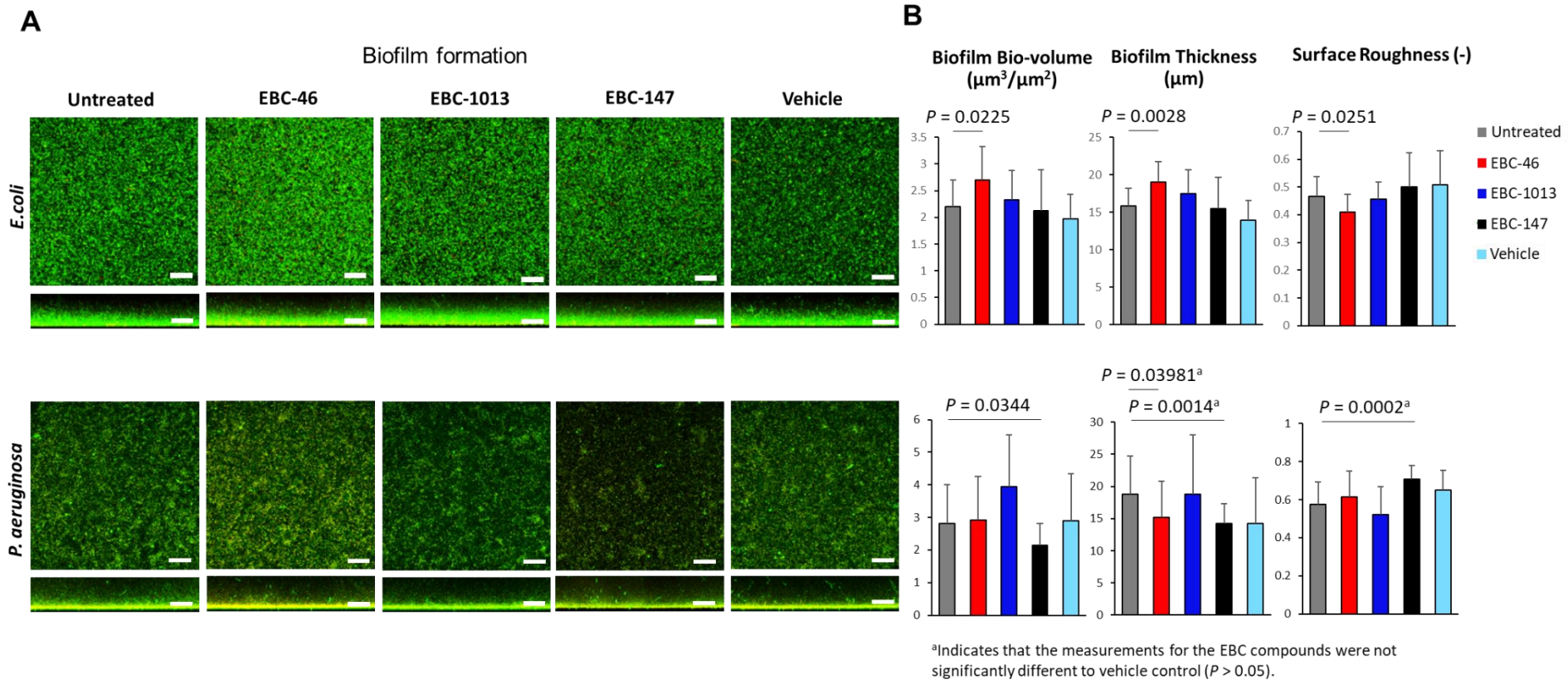

[a]Indicates that the measurements for the EBC compounds were not significantly different to vehicle control ($P > 0.05$).

Fig. S3. **The effect of epoxy-tiglianes treatment on biofilm formation in Gram-negative bacteria**. **(A)** Biofilm formation CLSM images (scale bar, 30 μm) and (**B**) COMSTAT image analysis (biofilm bio-volume, thickness and surface roughness) of *P. aeruginosa* PAO1 and *E. coli* IR57 following treatment with 256 μg/ml EBC-46, EBC-1013, EBC-147 alongside the untreated and vehicle controls (n≥3). Data shown as mean ±SD. Statistical comparisons were made using Kruskal-Wallis test and Mann-Whitney U multiple comparison tests. [a]Indicates that the measurements for the EBC compounds were not significantly different to the vehicle control ($P > 0.05$).

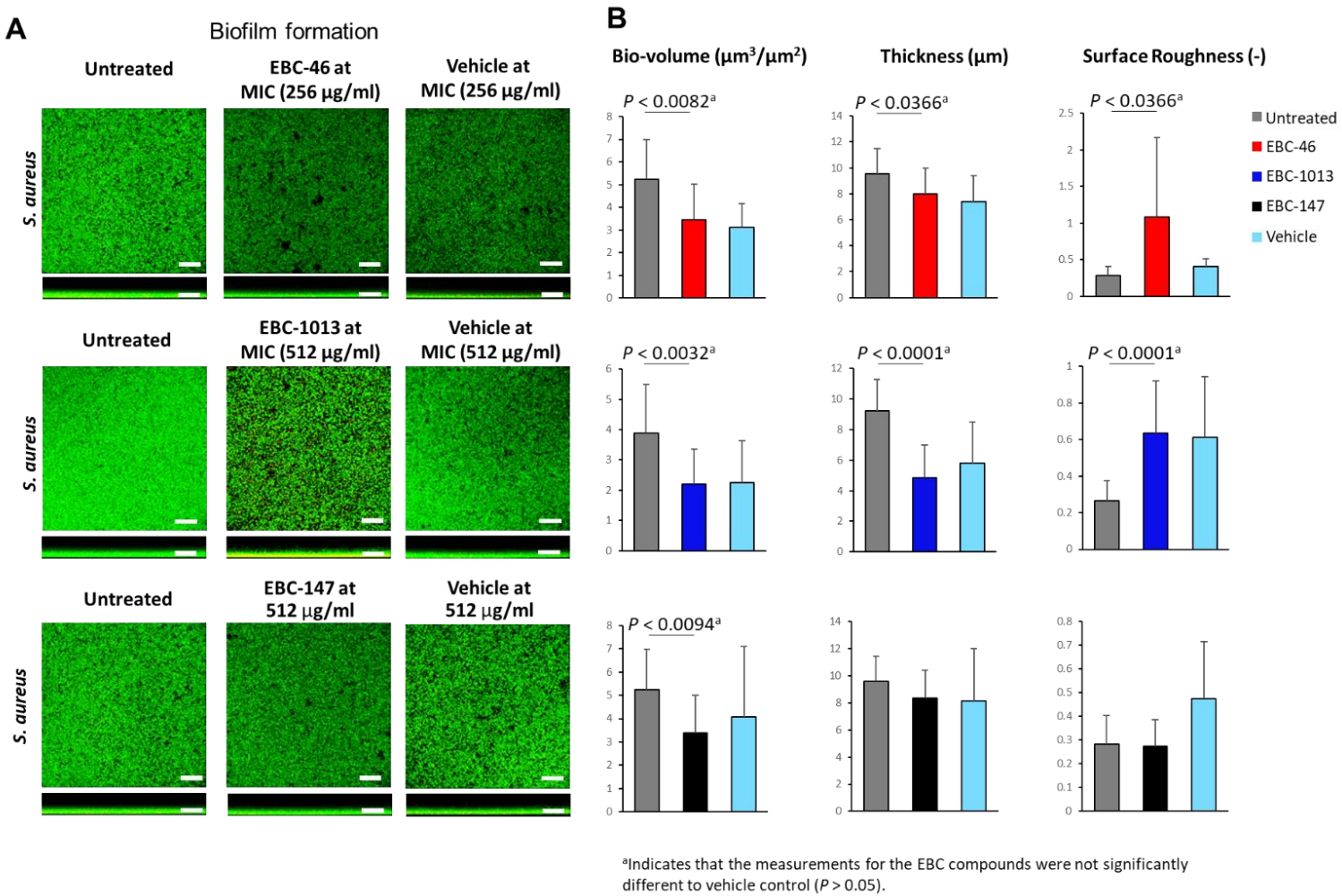

[a]Indicates that the measurements for the EBC compounds were not significantly different to vehicle control ($P > 0.05$).

Fig. S4. The effect of epoxy-tiglianes treatment on biofilm formation in Gram-positive bacteria. (**A**) Biofilm formation CLSM images (scale bar, 30 μm) and (**B**) COMSTAT image analysis (biofilm bio-volume, thickness and surface roughness) of *S. aureus* (MRSA) 1004A following treatment with EBC-46, EBC-1013, EBC-147 (256 – 512 μg/ml) alongside untreated and vehicle controls (n=3). Data shown as mean ±SD. Statistical comparisons were made using Kruskal-Wallis test and Mann-Whitney U multiple comparison tests. [a]Indicates that the measurements for the EBC compounds were not significantly different to the vehicle control ($P > 0.05$).

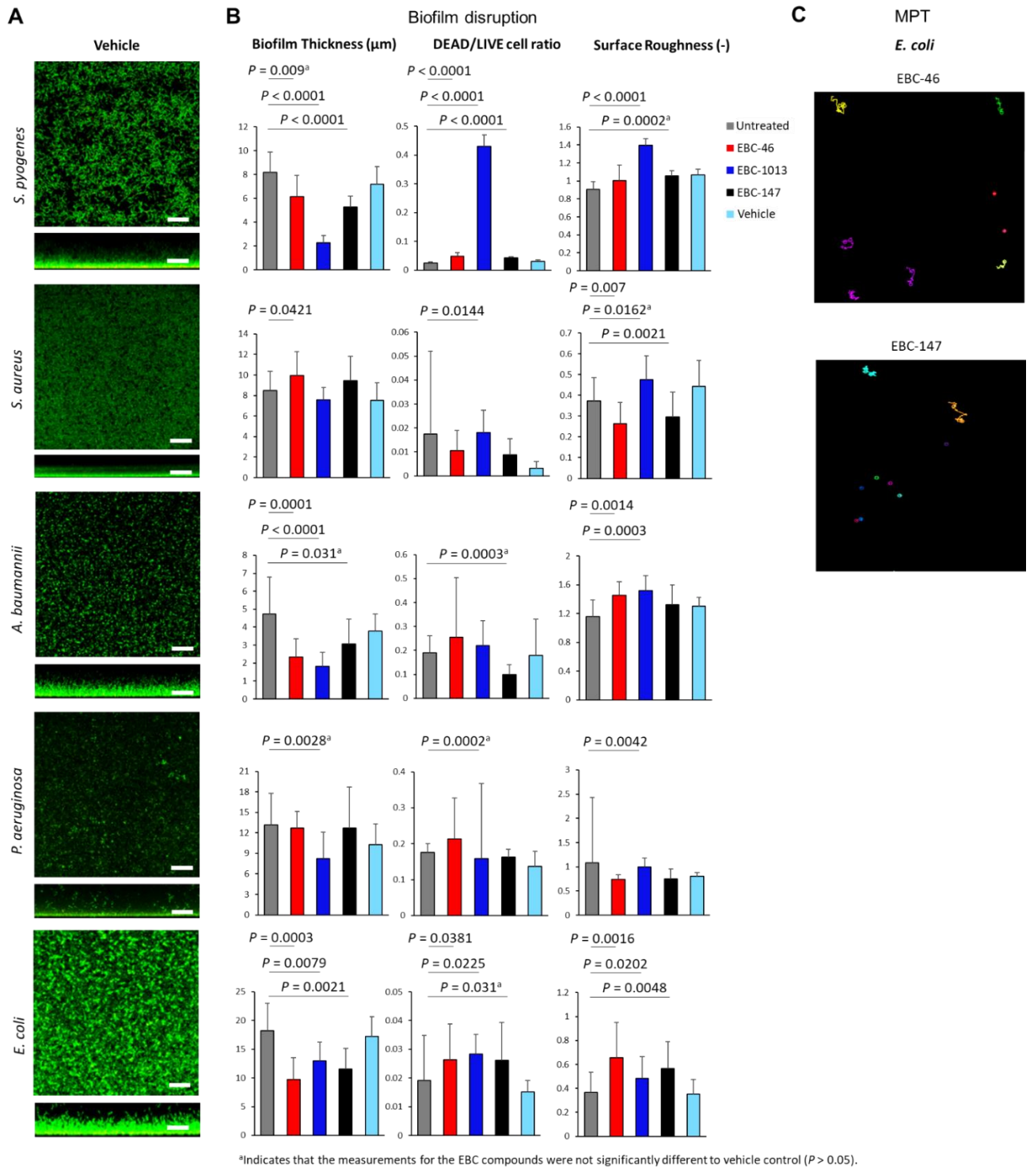

aIndicates that the measurements for the EBC compounds were not significantly different to vehicle control ($P > 0.05$).

Fig. S5. Epoxy-tiglianes induce disruption of established biofilms against a panel of wound isolates. (**A**) CLSM images showing biofilm disruption assay following treatment with vehicle control (equivalent to 256 µg/ml EBC treatment) against a panel of wound isolates including *S. pyogenes* E80*, S. aureus* (MRSA) 1004A, *A. baumannii* 7789*, P. aeruginosa* PAO1 and *E. coli* IR57 (scale bar, 30 µm). (**B**) Associated COMSTAT analysis (biofilm thickness, surface roughness and DEAD:LIVE cell ratio) showing biofilm disruption following treatment with 256 µg/ml EBC-46, EBC-1013, EBC-147 alongside untreated and vehicle control against the panel of wound isolates (n=3). Data shown as mean ±SD. Statistical comparisons were made using Kruskal-Wallis test and Mann-Whitney U multiple comparison tests. (**C**) Fluorescence microscopy images showing particle trajectories of 200 nm negatively charged carboxylate *Fluo*Spheres within EBC-46 and EBC-147 treated (256 µg/ml) *E. coli* IR57 biofilms, achieved using the MPT assay. [a]Indicates that the measurements for the EBC compounds were not significantly different to the vehicle control ($P > 0.05$).

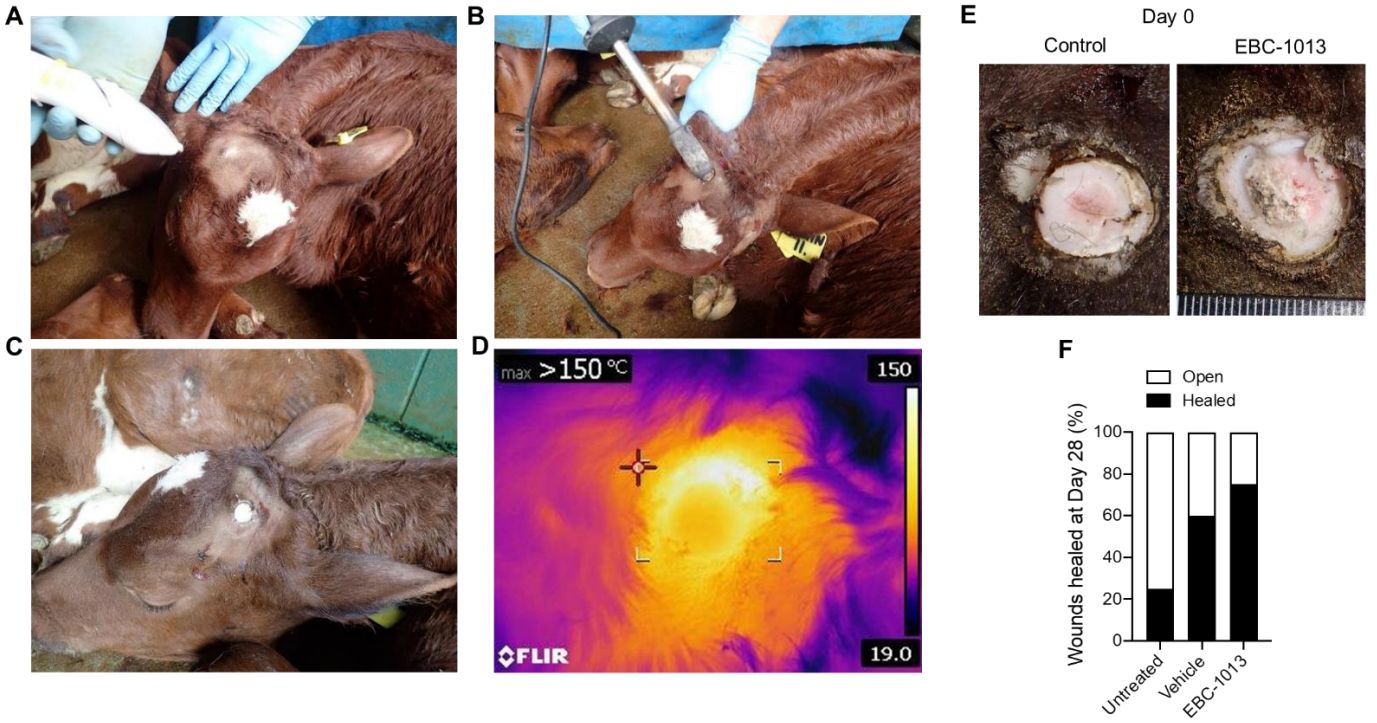
A
B
C
D
max >150 °C
150
19.0
FLIR
E
Day 0
Control
EBC-1013
F
Open
Healed
Wounds healed at Day 28 (%)
100
80
60
40
20
0
Untreated
Vehicle
EBC-1013
G
Day 0
Day 7
Day 14
Score
5
4
3
2
1
0
Ulceration
Granulation Tissue
New Collagen
Neutrophils
Chronic Inflammatory Cells
Bacteria
Untreated
Vehicle
EBC-1013

Fig. S6. EBC-1013 induced healing in acute thermal burn injury calf wound model. Photographs of (**A**) clipping of the hair, sedation and local anaesthetic nerve block. (**B** and **C**) Calf disbudding using a disbudding iron (at 500℃) creating bilateral, full-thickness burn wounds. (**D**) Image of disbudding site immediately following removal of disbudding iron showing localized area of the burn. (**E**) Day 0 wound images +/- EBC-1013 treatment (3 mg/ml) in the calf wound model. (**F**) Percentage of wounds healed at day 28 within the calf wound model (n=12). (**G**) Histology scores from wound biopsies at day 0, 7 and 14 demonstrating ulceration, granulation tissue, new collagen, neutrophils, chronic inflammatory cells and bacteria. Data shown as mean ±SEM.

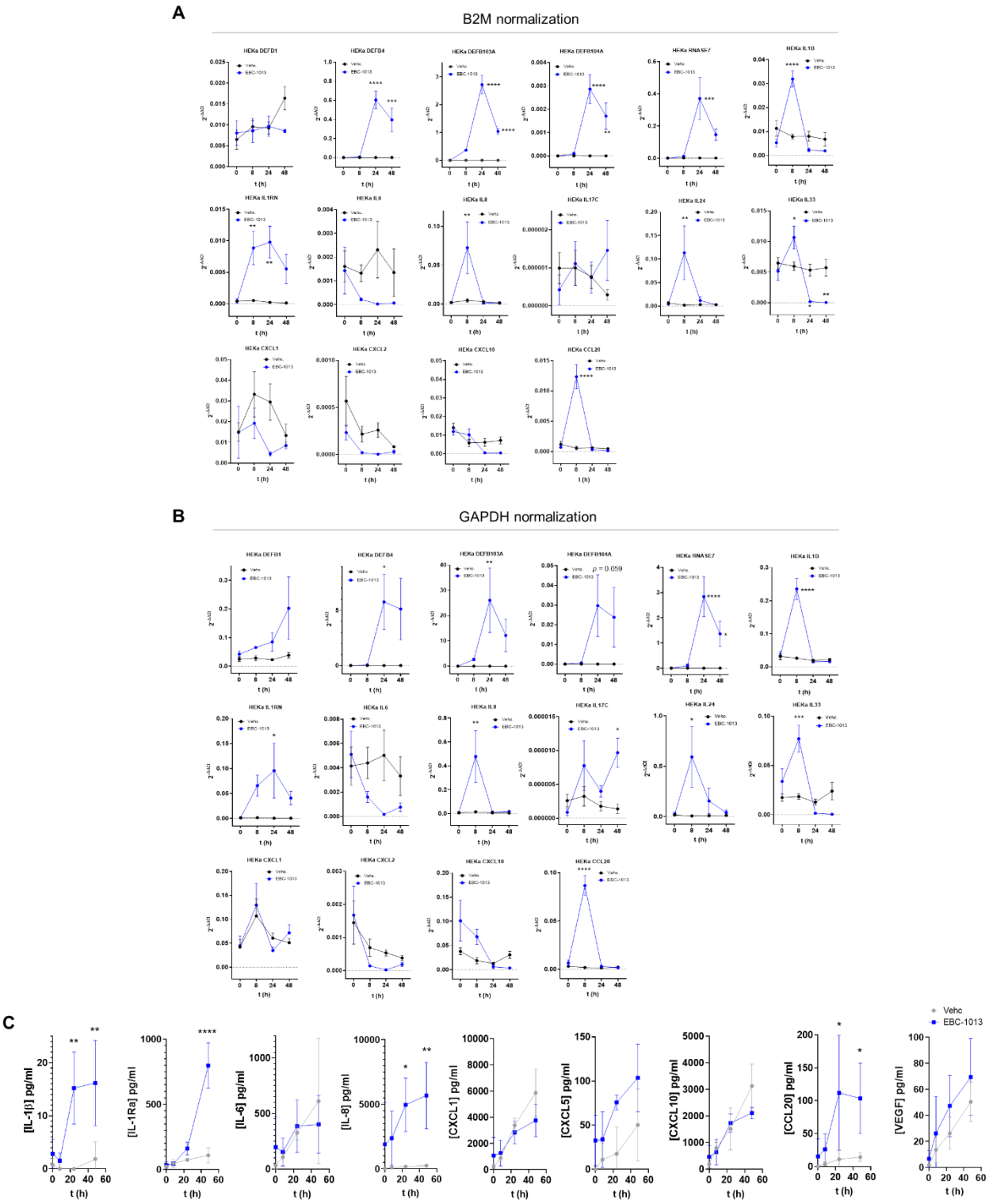
A
B2M normalization
HEKa DEFB1
HEKa DEFB4
HEKa DEFB103A
HEKa DEFB104A
HEKa RNASE7
HEKa IL1B
HEKa IL1RN
HEKa IL6
HEKa IL8
HEKa IL17C
HEKa IL24
HEKa IL33
HEKa CXCL1
HEKa CXCL2
HEKa CXCL10
HEKa CCL20
B
GAPDH normalization
p = 0.059
C
Vehc
EBC-1013
[IL-1β] pg/ml
[IL-1Ra] pg/ml
[IL-6] pg/ml
[IL-8] pg/ml
[CXCL1] pg/ml
[CXCL5] pg/ml
[CXCL10] pg/ml
[CCL20] pg/ml
[VEGF] pg/ml
t (h)

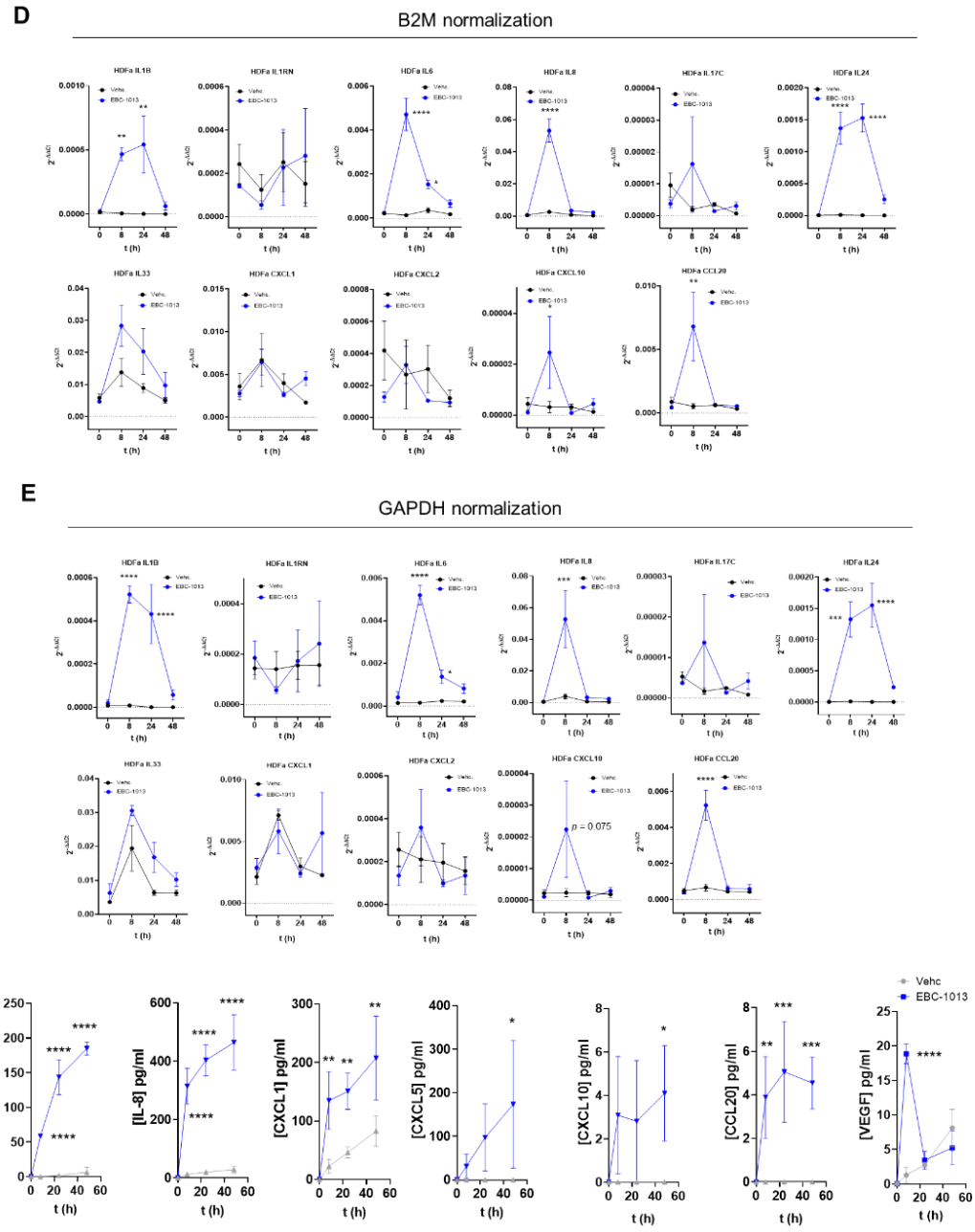
D
B2M normalization
HDFa IL1B
HDFa IL1RN
HDFa IL6
HDFa IL8
HDFa IL17C
HDFa IL24
HDFa IL33
HDFa CXCL1
HDFa CXCL2
HDFa CXCL10
HDFa CCL20
Vehc.
EBC-1013
t (h)
E
GAPDH normalization
HDFa IL1B
HDFa IL1RN
HDFa IL6
HDFa IL8
HDFa IL17C
HDFa IL24
HDFa IL33
HDFa CXCL1
HDFa CXCL2
HDFa CXCL10
HDFa CCL20
p = 0.075
Vehc.
EBC-1013
t (h)

F
[IL-6] pg/ml
[IL-8] pg/ml
[CXCL1] pg/ml
[CXCL5] pg/ml
[CXCL10] pg/ml
[CCL20] pg/ml
[VEGF] pg/ml
Vehc
EBC-1013
t (h)

Fig. S7. Data used for generation of qPCR and LEGENDplex heatmaps detailed in Fig. 7. Time versus. $2^{-\Delta\Delta Ct}$ graphs acquired from HEKa cells for the indicated transcripts (**A**) *B2M* normalization; n=3 and (**B**) *GAPDH* normalization; n=3. Data shown as mean ±SEM. (**C**) LEGENDplex quantification of the indicated cytokines/chemokines released in response to vehicle/EBC-1013 treatment of HEKa (100ng/ ml; n=3). Data shown as mean ±SD. Time versus. $2^{-\Delta\Delta Ct}$ graphs acquired from HDFa cells for the indicated transcripts (**D**) *B2M* normalization; n=3 and (**E**) *GAPDH* normalization; n=3. Data shown as mean ±SEM. (**F**) LEGENDplex quantification of the indicated cytokines/chemokines released in response to vehicle/EBC-1013 treatment of HDFa cells (100 ng/ml; n=3). Data shown as mean ±SD. (Data from **A** and **D** was used to generate the qPCR heatmap data depicted in Fig. 7). *P* values were calculated by 2-way ANOVA with Sidak's correction (* $P < 0.05$, ** $P < 0.01$, *** $P < 0.001$, **** $P < 0.0001$). (Data from **C** and **F** was used to generate the LEGENDplex heatmap data depicted in Fig. 7).

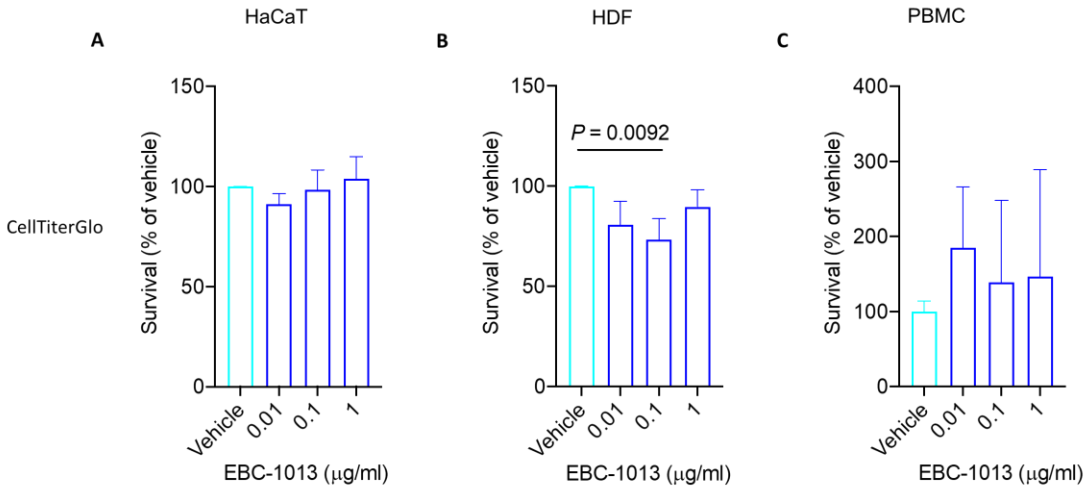
A
HaCaT
B
HDF
C
PBMC
CellTiterGlo
Survival (% of vehicle)
150
100
50
0
P = 0.0092
400
300
200
Vehicle
0.01
0.1
1
EBC-1013 (μg/ml)

Fig. S8. The effect of EBC-1013 on keratinocyte, fibroblast and PBMC cellular viability. HaCaT (**A**), HDF (**B**) and PBMC (**C**) cells were treated with vehicle or the indicated concentrations of EBC-1013. ATP concentration (CellTiterGlo) was determined after 72 h for all cell types (n=3). Data shown as mean ±SD. Statistical comparisons were made using one-way ANOVA with Dunnett's correction.

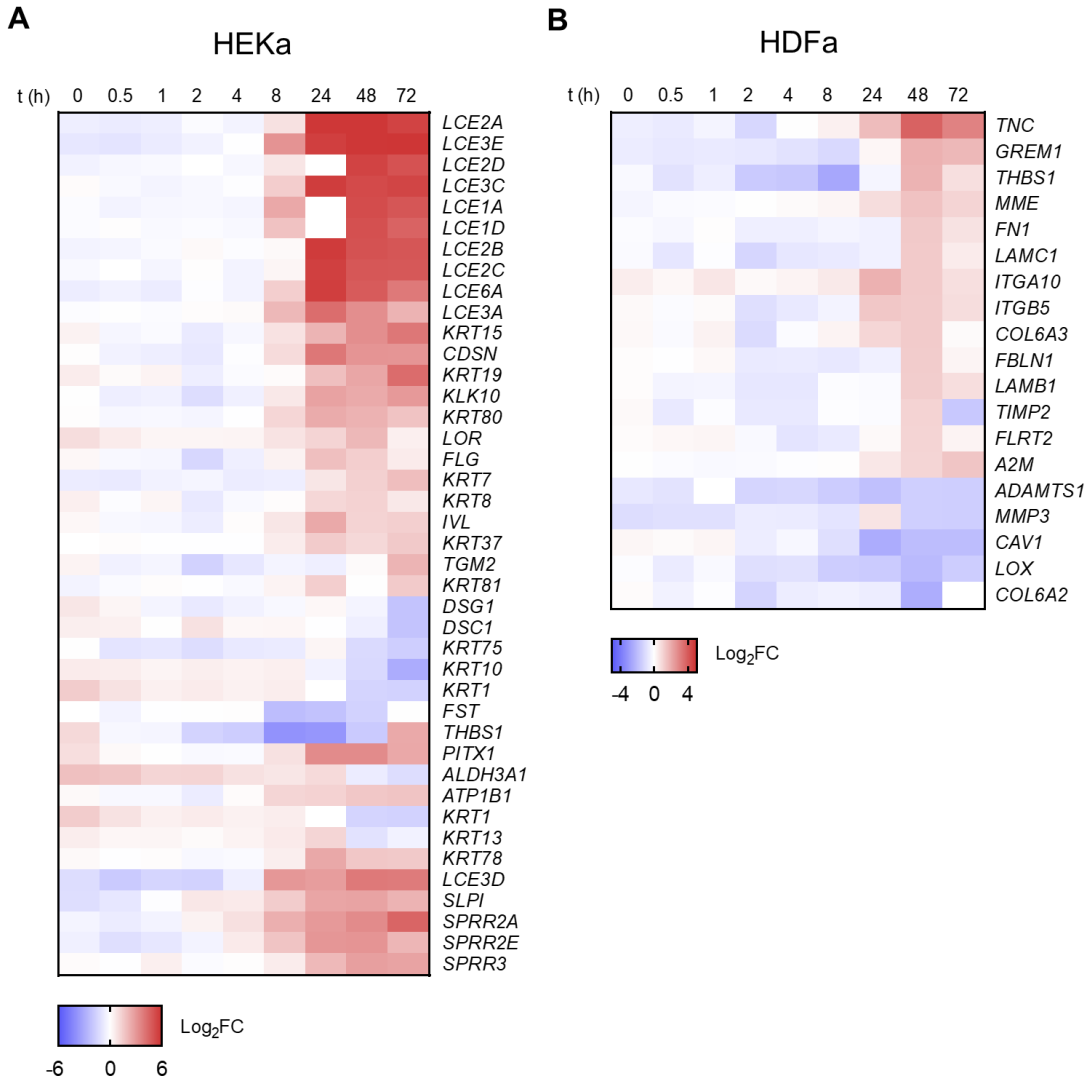
A
HEKa
t (h) 0 0.5 1 2 4 8 24 48 72
LCE2A
LCE3E
LCE2D
LCE3C
LCE1A
LCE1D
LCE2B
LCE2C
LCE6A
LCE3A
KRT15
CDSN
KRT19
KLK10
KRT80
LOR
FLG
KRT7
KRT8
IVL
KRT37
TGM2
KRT81
DSG1
DSC1
KRT75
KRT10
KRT1
FST
THBS1
PITX1
ALDH3A1
ATP1B1
KRT1
KRT13
KRT78
LCE3D
SLPI
SPRR2A
SPRR2E
SPRR3
Log2FC
-6 0 6
B
HDFa
t (h) 0 0.5 1 2 4 8 24 48 72
TNC
GREM1
THBS1
MME
FN1
LAMC1
ITGA10
ITGB5
COL6A3
FBLN1
LAMB1
TIMP2
FLRT2
A2M
ADAMTS1
MMP3
CAV1
LOX
COL6A2
Log2FC
-4 0 4

Fig. S9. Gene sets associated with skin development and extracellular matrix organization GO signatures in HEKa and HDFa cells. (**A**) Heat map representation of selected targets in HEKa expression profiling data from the "skin development" GO pathway. (**B**) Heat map representation of selected targets in HDFa expression profiling data from the "extracellular matrix organization" GO pathway.

A

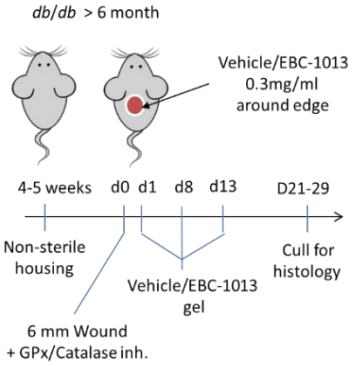
db/db > 6 month
Vehicle/EBC-1013
0.3mg/ml
around edge
4-5 weeks
d0
d1
d8
d13
D21-29
Non-sterile
housing
Cull for
histology
Vehicle/EBC-1013
gel
6 mm Wound
+ GPx/Catalase inh.

B

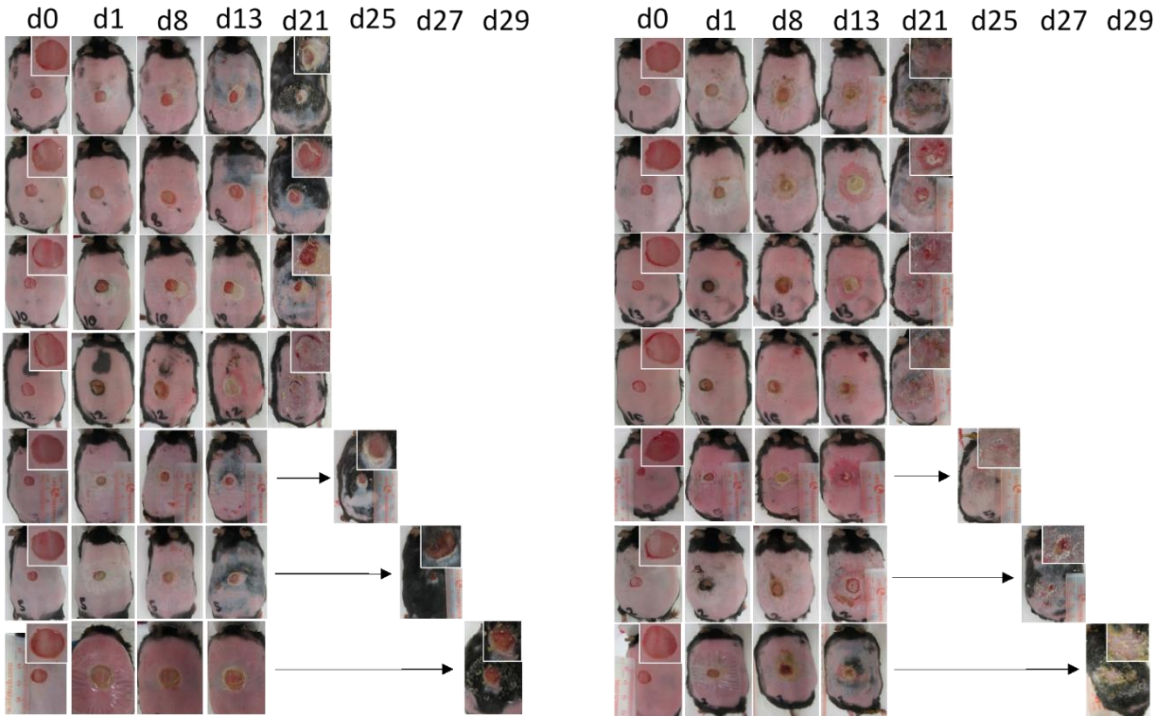
d0
d1
d8
d13
d21
d25
d27
d29
d0
d1
d8
d13
d21
d25
d27
d29

Fig. S10. EBC-1013 induced healing in a diabetic mouse model of chronic wounds. (**A**) Schematic of the wounding/treatment procedure in the *db/db* diabetic mouse model. (**B**) Images of skin wounds in *db/db* mice (n=7) treated with vehicle (left) or EBC-1013 (0.3 mg/ml; right) taken on days 0, 1, 8, 13 and 21-29 (end day). Mice were treated on days 1, 8 and 13.

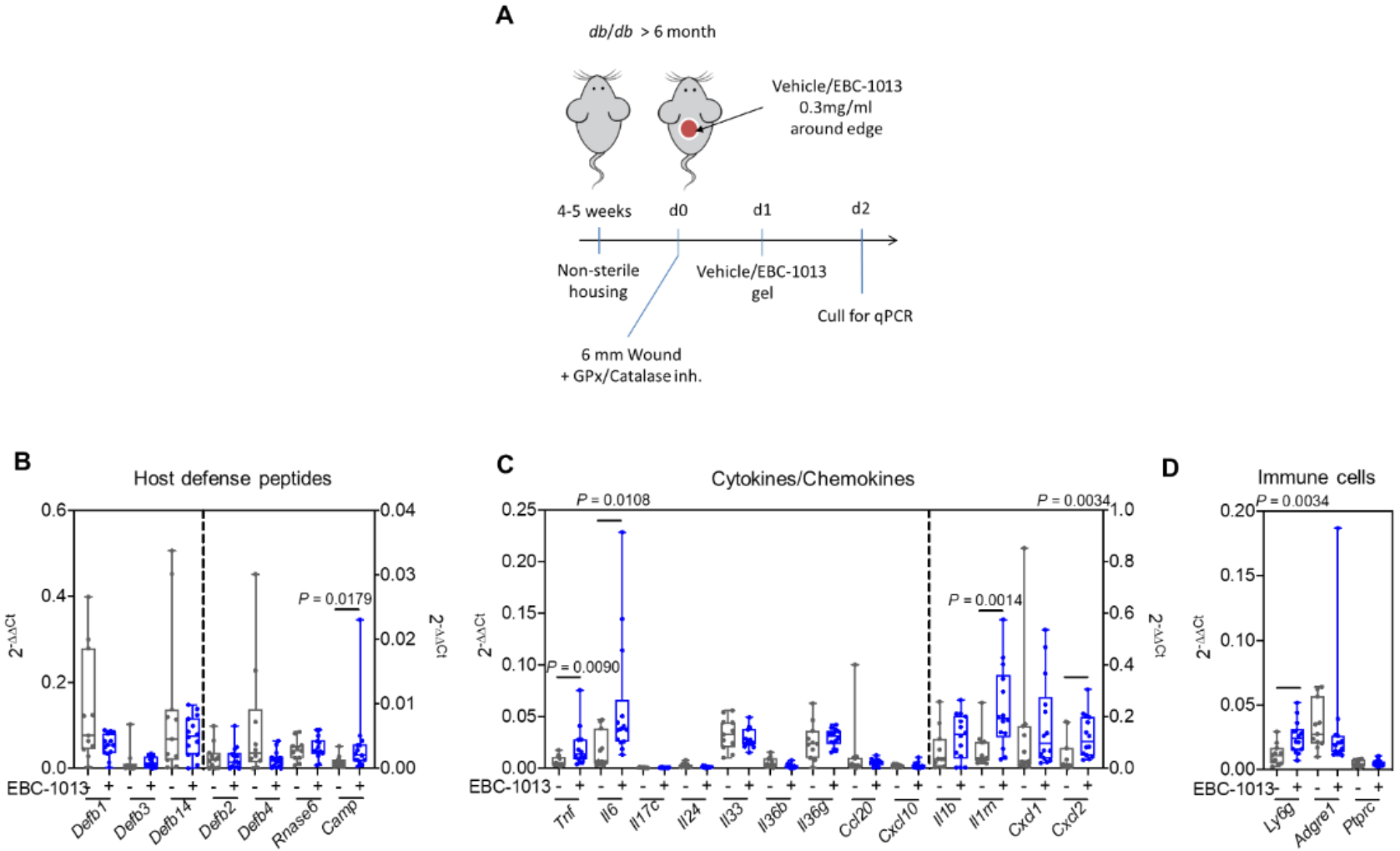
A
db/db > 6 month
Vehicle/EBC-1013
0.3mg/ml
around edge
4-5 weeks
d0
d1
d2
Non-sterile
housing
Vehicle/EBC-1013
gel
Cull for qPCR
6 mm Wound
+ GPx/Catalase inh.
B
Host defense peptides
P = 0.0179
EBC-1013
Defb1
Defb3
Defb14
Defb2
Defb4
Rnase6
Camp
C
Cytokines/Chemokines
P = 0.0108
P = 0.0034
P = 0.0090
P = 0.0014
Tnf
Il6
Il17c
Il24
Il33
Il36b
Il36g
Ccl20
Cxcl10
Il1b
Il1rn
Cxcl1
Cxcl2
D
Immune cells
P = 0.0034
Ly6g
Adgre1
Ptprc

Fig. S11. Analysis of target gene changes in mouse samples using *Gapdh* mRNA as normalization. (**A**) Schematic of treatment approach for the isolation of wounds in preparation for RNA extraction and qPCR analysis. Additional qPCR analysis data of treated wounds revealing changes in (**B**) host-defense peptides, (**C**) cytokines/chemokines and (**D**) PMNL marker expression following EBC-1013 treatment (0.3 mg/ml). RNA acquired from vehicle- and EBC-1013-treated wounds (24 h) was analyzed using primers for the indicated gene sets. Data are expressed as $2^{-\Delta\Delta Ct}$ values. *Gapdh* mRNA was used as the normalization control. (Additional analysis with *B2m* normalization can be seen in Fig. 8). Vehicle, - (n=11); EBC-1013, + (n=14). The data is presented as a box-and-whisker plot where the boxes encompass the 25^{th} to 75^{th} percentile, the line is at the median, the whiskers represent the range and the dots are the individual data points. *P* values (indicated above relevant comparisons) were calculated by Mann-Whitney U Test.

Table S1. Physicochemical properties of various epoxy-tigliane compounds (calculated using the Swiss ADME computational chemistry website [swissadme.ch] unless otherwise stated; *64*).

Compounds	Formula	Molecular weight (g/mol)	Log *P*	Log *P*[a]	H-bond donor	H-bond acceptor	Total polar surface Area ($A^{\circ 2}$)	Molar refractive	Log *S*
EBC-1013[b]	$C_{32}H_{48}O_{10}$	592.72	2.37	3.47[c]	4	10	163.12	153.29	-4.78
EBC-46[d]	$C_{30}H_{42}O_{10}$	562.64	1.23	2.91	4	10	163.12	143.20	-4.15
EBC-147	$C_{28}H_{40}O_{10}$	536.61	0.67	2.68	4	10	163.12	134.06	-3.53

[a]Experimentally derived Log *P* values (following protocol outlined in Cullen et al 2021; *18*). [b]Semi-synthetic, C12 C13 dihexanoate. [c]This study. [d]Prototypical epoxy-tigliane. *Log P*, octanol–water partition coefficient (lipophilicity). Log *S*, aqueous solubility.

Table S2. Minimum inhibitory concentration assays (MICs) determined for epoxy-tigliane compounds. EBC-46, EBC-1013 and EBC-147 compounds tested against Gram-positive *S. pyogenes* E80 and *S. aureus* (MRSA) 1004A, and Gram-negative *A. baumannii* 7789, *P. aeruginosa* PAO1 and *E. coli* IR57 strains.

Compound	MIC (µg/ml) for epoxy-tigliane compounds				
	S. aureus **1004A**	***S. pyogenes*** **E80**	***E. coli*** **IR57**	***P. aeruginosa*** **PAO1**	***A. baumannii*** **7789**
EBC-46[a]	256	128	>512	>512	>512
EBC-1013	512	256	>512	>512	>512
EBC-147	>512	>512	>512	>512	>512

[a]Prototypical epoxy-tigliane.

Table S3. **Diffusion coefficients of 200 nm FluoSphere particles in EBC treated *E.coli* IR57 biofilms.** Diffusion coefficients <Deff> (cm^2/s x 10^{-9}) of 200 nm negatively charged carboxylate modified FluoSphere particles in EBC-treated *E.coli* IR57 biofilms (256 µg/ml; 72 h) measured using the MPT assay. Biofilms treated with 256 µg/ml EBC-46, -1013, -147 and untreated and vehicle controls (n=3).

	Untreated	**EBC-46**	**EBC-1013**	**EBC-147**	**Vehicle[a]**
Diffusion Coefficient (cm^2/s x 10^{-9})	0.0044 ± 0.0014	0.6018 ± 0.0901	0.8449 ± 0.1250	0.1607 ± 0.0104	0.0155 ± 0.0052
***P* value[b]**		0.0001	0.0001	0.0934	0.9999

[a]Vehicle (ethanol) equivalent control**.** [b]Statistical comparison to the control. Data expressed as mean ± SD. Statistical comparisons were made using a one-way ANOVA and Tukey's multiple comparison tests.

Table S4. Primers used in HEKa/HDFa based qPCR experiments. All primers were designed using PrimerQuest (Integrated DNA Technologies).

Gene	Primer	Sequence (5'-3')
DEFB1	DEFB1_F	TCTGCTGTTTACTCTCTGCTTAC
	DEFB1_R	GGCAGGCAGAATAGAGACATT
DEFB2	DEFB2_F	GCCATGAGGGTCTTGTATCTC
	DEFB2_R	CAGGTAACAGGATCGCCTATAC
DEFB103A	DEFB103A_F	CTTCTGTTTGCTTTGCTCTTCC
	DEFB103A_R	CGCCTCTGACTCTGCAATAAT
DEFB104A	DEFB104A_F	GAAATGTCGCAGCCAAGAATAC
	DEFB104A_R	CGATTCAGTAAGCTCTCATCCC
RNASE7	RNASE7_F	GGACAGAGTCCTTTAGGTTTCC
	RNASE7_R	GAAGAGAATGCTCTGGGTGTAG
IL1B	IL1B_F	GGTGTTCTCCATGTCCTTTGTA
	IL1B_R	GCTGTAGAGTGGGCTTATCATC
IL1RN	IL1RN_F	CTGTGTCAAGTCTGGTGATGAG
	IL1RN_R	CACTGTCTGAGCGGATGAAG
IL6	IL6_F	CACTCACCTCTTCAGAACGAAT
	IL6_R	GCTGCTTTCACACATGTTACTC
IL8	IL8_F	AAATCTGGCAACCCTAGTCTG
	IL8_R	GTGAGGTAAGATGGTGGCTAAT
IL17C	IL17C_F	TCCATCTCACCCTGGAGATAC
	IL17C_R	GTGCATCGATACAGCCTCTG
IL24	IL24_F	TTCTCTGGAGCCAGGTATCA
	IL24_R	AGAAGGCTTCCCACAGTTTC
IL33	IL33_F	GTGACGGTGTTGATGGTAAGA
	IL33_R	CTCCACAGAGTGTTCCTTGTT
IL36B	IL36B_F	GCATAAACCTGGATGTGAGAGA
	IL36B_R	CCTTCTTCCTGAGATGGTGATG
IL36G	IL36G_F	AGGAGAGCTGGGTGGTATAA
	IL36G_R	AAAGCTCAGTGTTTGGTCTTTG
CXCL1	CXCL1_F	GCTGAACAGTGACAAATCCAAC
	CXCL1_R	GCTGTGTCTCTCTTTCCTCTTC
CXCL2	CXCL2_F	GCATCGCCCATGGTTAAGA
	CXCL2_R	TCAGGAACAGCCACCAATAAG
CXCL10	CXCL10_F	AGCTCTACTGAGGTGCTATGT
	CXCL10_R	GTACCCTTGGAAGATGGGAAAG
CCL20	CCL20_F	GGACATAGCCCAAGAACAGAAA
	CCL20_R	GTCCAGTGAGGCACAAATTAGA
GAPDH	GAPDH_F	GGCTCTCCAGAACATCATCCCTGC
	GAPDH_R	GGGTGTCGCTGTTGAAGTCAGAGG
B2M	B2M_F	ATGTCTCGCTCCGTGGCCTTA
	B2M_R	ATCTTGGGCTGTGACAAAGTC

Table S5. Primers used in *db/db* wound based qPCR experiments. All primers were designed using PrimerQuest (Integrated DNA Technologies).

Gene	Primer	Sequence (5'-3')
Defb1	Defb1_F	CTCCAGCTGCCCATCTAATAC
	Defb1_R	ATCCATCGCTCGTCCTTTATG
Defb2	Defb2_F	AGCCATTTGTCCTCCTTCTG
	Defb2_R	GACTTCCATGTGCTTCCTTCTA
Defb3	Defb3_F	TTGAGGAAAGGAGGCAGATG
	Defb3_R	CGGGATCTTGGTCTTCTCTATTT
Defb4	Defb4_F	CGAAGAACCAGCAAGATGAATAAA
	Defb4_R	CTAGAACTGGAGTTAGAGAAGGTAATC
Defb14	Defb14_F	GCCTTGGAAAGGAAGAACAAATAG
	Defb14_R	CCCTCACCCTGCATATTCTAAG
Rnase6	Rnase6_F	GCGCGGTGTCAACAATTATAC
	Rnase6_R	CAGTTCTTCCGACCGTTCTT
Camp	Camp_F	TCCCTAGACACCAATCTCTACC
	Camp_R	GCCACATACAGTCTCCTTCAC
Il1b	Il1b_F	GGTACATCAGCACCTCACAA
	Il1b_R	TTAGAAACAGTCCAGCCCATAC
Il1rn	Il1rn_F	TTGTGCCAAGTCTGGAGATG
	Il1rn_R	CTCAGAGCGGATGAAGGTAAG
Il6	Il6_F	GATAAGCTGGAGTCACAGAAGG
	Il6_R	TTGCCGAGTAGATCTCAAAGTG
Il17c	Il17c_F	CTTGGGAGGAAATGGGTGTT
	Il17c_R	AGTAGGCAACCAGCCTAGAA
Il24	Il24_F	GTCTTGAGGTCATTCTCCACTC
	Il24_R	CTGGTGTGCACTCTCACTAAT
Il33	Il33_F	TCCACGGGATTCTAGGAAGA
	Il33_R	GAGGCAGGAGACTGTGTTAAA
Il36b	Il36b_F	TGTGGGAACCGAATCATAACA
	Il36b_R	AGTCAGGACCCATACCATCT
Il36g	Il36g_F	AGGTAAGCAGGACCAACATTAT
	Il36g_R	GAGAACATCCTTACACCACTCC
Cxcl1	Cxcl1_F	GTGTCTAGTTGGTAGGGCATAAT
	Cxcl1_R	CAGTCCTTTGAACGTCTCTGT
Cxcl2	Cxcl2_F	AGAGGGTGAGTTGGGAACTA
	Cxcl2_R	GCCATCCGACTGCATCTATT
Cxcl10	Cxcl10_F	CAGTGGATGGCTAGTCCTAATTG
	Cxcl10_R	GACCATGGCTTGACCATCAT
Ccl20	Ccl20_F	TGAACCTCCTCAGCCTAAGA
	Ccl20_R	CCCAGCTGTGATCATTTCCT
Ly6g	Ly6G_F	AACCTGGTCAGAGAGGAAGT
	Ly6G_R	CACACAGTAGGACCACAAGAAG
Adgre1	Adgre1_F	TACCACTTGCCCAGCTTATG
	Adgre1_R	GGGCCTTGAAAGTTGGTTTG
Cd45	Cd45_F	CCCTTCTTCTGCCTCAAAGT

	Cd45_R	CACCTGGATGATATGTGGTCTC
B2m	B2M_F	TTCTGGTGCTTGTCTCACTGA
	B2M_R	CAGTATGTTCGGCTTCCCATTC
Gapdh	GAPDH_F	AGGTCGGTGTGAACGGATTTG
	GAPDH_R	GGGGTCGTTGATGGCAACA